SULI Report: Further FRC work in UEDGE and LSP

Alan Kaptanoglu[1]

[1]Princeton Plasma Physics Laboratory
*Corresponding author: alank2@alumni.stanford.edu

Abstract

The field-reversed configuration (FRC) is being considered for use as a fusion device and as a direct fusion-drive rocket engine for future space missions. We have used a 2D fluid code, UEDGE, to conduct numerical simulations of an FRC scrape-off-layer (SOL) region. Previous work examined the FRC suitability as a rocket engine in UEDGE. This work extends that by examining the FRC suitability as a fusion device. Furthermore, it extends the previous analysis by allowing new magnetic geometry shapes, improved grid resolution and a prescription for quickly converging FRC-like solutions in UEDGE. A gradient descent method was made to match experimental diagnostics. Work was also done in the 3D kinetic code, LSP, to examine FRC formation in the core of the FRC. We compare even and odd parity RMF penetration and examine a new antenna design.

1 Introduction

This is the research report paper required as part of the spring 2017 SULI program. My goal with this report is to introduce future students to this research project, so that any students whose work will build upon this project will understand the project and it's results. The intended audience of this report is either a new summer intern or a graduate student. For any clarifications or help, please feel free to email kaptanoglualan@gmail.com.

2 The FRC

The field-reserved configuration (FRC) is being studied for use as a fusion reactor. The FRC has many advantages relative to other reactor designs, including compact size, smaller neutron flux, high β, and potential as a rocket engine.

Figure 1 shows a schematic of an FRC. The closed field lines in the center of figure 1 are the core. In this case, the closed field lines are generated by odd-parity rotating magnetic fields. The open field lines surrounding the core are known as the scrape-off layer (SOL). Fusion power is generated in the core of the FRC. Some of this energy is deposited into the SOL – mostly uniformly through energetic ions in betatron orbits, but also through radial heat flux from hot ions in normal cyclotron orbits at the interface between the core and SOL. If used as a rocket, the FRC would have a box to the left of the reactor where cold gas is puffed into the machine. This gas will eventually become ionized, flow through the SOL, and out a magnetic nozzle on the other side of the machine.

3 UEDGE

UEDGE is a 2D multi-species fluid code used to model the SOL region of fusion reactors. UEDGE finds a steady-state self-consistent solution to continuity equations, momentum equations, and energy equations for each species. The equations and transport coefficients are taken from Braginskii (Braginskii, 1965). UEDGE also calculates ionization and recombination rates, and has scripts to calculate the flow of power and particles in a simulation.

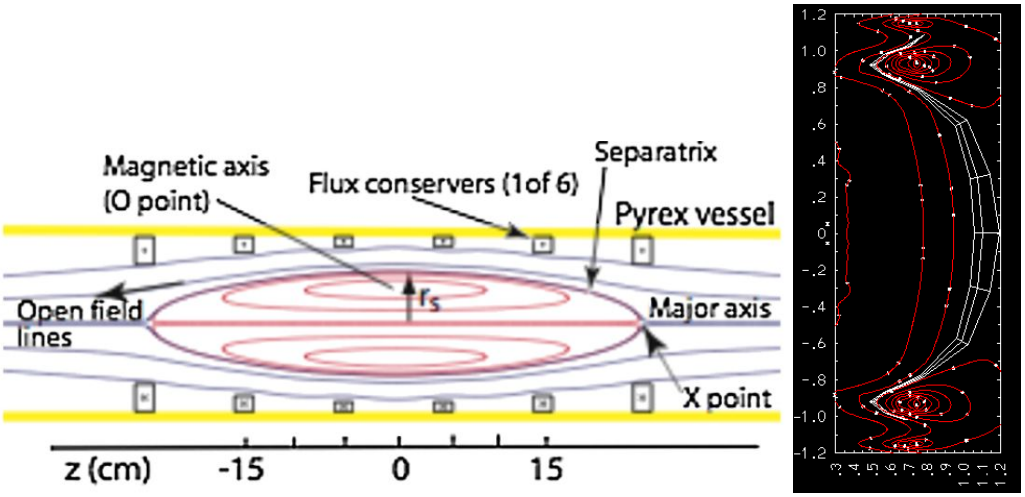

Figure 1: Left: The R-Z plane showing the FRC geometry. Right: The R-Z plane displaying the magnetic flux contours in red and the generated UEDGE grid in white.

3.1 Magnetic Geometry

However, for a long time, there was no general prescription for changing the magnetic geometry of the simulation. Because UEDGE solves the equations along field lines, this is a serious problem if one wants to try converge a new magnetic geometry from scratch, increase the grid resolution, or introduce any other desirable grid features. Fortunately, Gingred (Olivier Izacard, 2017) has been developed, which takes a GEQDSK file and converts it into a grid of arbitrary resolution that UEDGE can use. My earliest work was to convert the magnetic geometry written out by the RMF code into the GEQDSK file format. This python file is provided and can easily be changed to write other formats to GEQDSK. This allows future work for an in depth analysis of how the grid and magnetic geometry affect the SOL.

3.2 Boundary Conditions

For the PFRC device simulated previously as a rocket, typical boundary conditions are as follows. (McGreivy, 2016) The right boundary is an open boundary where particles are allowed to flow unimpeded out of the simulation, and gradients in density and temperature are zero. This is physically applicable to an FRC rocket, where the boundary at the magnetic nozzle is the vacuum of space.

The left boundary represents one wall of the gas box wall. Here, 99.9% of the incoming deuterium ions and atomic deuterium is recycled off the wall as molecular deuterium. The molecular gas temperature is assumed a constant of $T = 0.1$ eV but the atomic gas, electron, and ion temperatures are calculated self consistently. The thermal flux and (ionization) potential energy of the plasma ions are deposited onto the gas box walls. The plasma is allowed to stream freely to the wall, but the atomic deuterium is constrained to have some fraction ($\frac{1}{2}$ to $\frac{1}{10}$) of the velocity of the plasma at the wall.

Since the FRC core consists of closed field lines with ions with small gyro-orbits, physically one would expect the gradient and flux of all quantities at the center boundary to be small. We can approximate this by setting the derivatives of temperature and density at the core to be zero.

The top boundary represents the plasma-facing materials at the top of the gas box as well as outside the FRC core. Here, all of the plasma and atomic deuterium hitting the top wall was recycled as molecular deuterium. An albedo of 0.5 was also set, meaning that the incoming atomic deuterium flux was reduced by a factor of 2. Zero temperature and velocity gradients were set at this boundary. Charged particle transport to the these walls is negligible owing, in large part, to the rapid axial flow.

However, converging solutions from scratch (necessary if one wants to use a new magnetic geometry or pretty much change the grid in any way) is made far, far easier by changing all the density and temperature boundary conditions to specify values (Dirichlet boundary conditions). We spent quite a bit of time trying to figure out how to converge things with $\frac{dn_{e/i}}{dr} = 0$, $\frac{dT_{e/i}}{dr} = 0$ (Neumann boundary conditions) and it is

extremely difficult, especially with particle and power sources. Once one has convergence with Dirichlet boundary conditions with no external (not including the boundaries) power source, one can usually quite easily change the solution back to Neumann boundary by boundary.

In order to simplify the geometry and make the simulations conducive to fitting experimental diagnostics, we also got rid of the "core" region so that the entire inner wall is a "private flux region". This is easier because currently a "core" region can only specify uniform power, temperature, and density in UEDGE. However, a "private flux region" can specify functions (rather than a single value) for temperature and density at this boundary and power sources can be input inside the simulation rather than as a boundary condition. This makes it more flexible and it can better fit experimental profiles.

For the simulations with recycling walls on both sides (simulating a first attempt at a "power plant") typical boundary conditions and parameters are the same as the rocket but with both left and right boundaries (divertor plates) with values for recycling $\approx$ 90% with a similar constraint on the velocity of the atomic deuterium. There is also a molecular gas sink that takes out gas after it has passed over the core region.

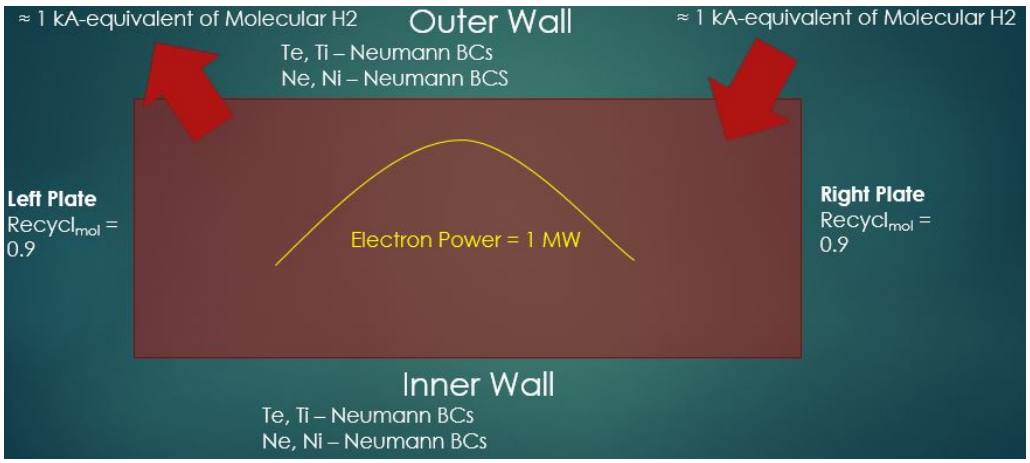

Figure 2: Boundary conditions and parameters for the UEDGE simulations

3.3 Work Flow

Example scripts to convert files to GEQDSK format, run uedge, plot uedge quantities, run a gradient descent method, and so on, are included in an OMFIT Meneghini et al. (2015) project available from myself or Dr. Cohen. A typical uedge work flow run outside OMFIT is (note that bash commands work in the uedge prompt if there is an exclamation point in front of the command):

1 Start up uedge with "./xuedge616"

2 Go to wherever the input file is with "!cd ..."

3 Read the grid input file with "read ingrid.b"

4 Read the uedge input file with "read rd1mw_1ka"

5 If not converged, "read rdinitdt" followed by "read rdcontdt". This will begin a loop at small timestep that attempts to converge the solution.

6 When close to numerical convergence, $F_{tolerance} \approx 1e-8$ with $\delta t > 1e-2$, then try to obtain the physical convergence of $F_{tolerance} \approx 1e-13$ with $\delta t \approx 1e20$. Usually this last part is easy and can be done by one "exmain".

7 Save the converged solution by "character *85 namefile = 'pf_myFavoriteFileName.pdb'" and "read ak_save_all". This outputs all the uedge variables into a file in data_rs/namefile.

8 Import the 'pf' file into OMFIT for plotting, gradient descent, power balance calculations, and so on.

3.3.1 Convergence Issues

As mentioned, it is often not easy to converge solutions in uedge, especially from scratch and with Neumann boundary conditions. There are some "oscillatory solutions" (metastable solutions) where the error gets stuck at some small value. This can be fixed by making δt and the tolerance smaller (bigger jumps around the parameter space) and trying to jump out of the metastable valley. Another frequent error is that the temperature or density of some species goes negative, causing uedge to crash. This almost always happens with Neumann boundary conditions. It can be avoided by using pure Dirichlet boundary conditions for temperature and density, verifying that the profiles in the radial and axial direction are smooth and roughly the expected order of magnitudes, and then slowly switching to Neumann boundary conditions.

3.4 Rocket

At the magnetic nozzle, the hot electrons setup an electric field in the nozzle, which accelerates the protons out the nozzle. Once it leaves the nozzle, the ejected plasma detaches from the magnetic field lines. Work has been done illustrating that the FRC could be a promising candidate for future space travel (McGreivy, 2016). While my work does not explore this parameter space further, it allows for fitting experimental diagnostics and changes to the magnetic geometry. Further work should use these new capabilities to explore the parameter space of rocket quantities like thrust.

3.5 Gasbox on both ends

In all the FRC UEDGE simulations there is a molecular gas source (flux) along the upper wall specified with total-width w_m, strength I_m (in kAmp-equivalents)

$$\Phi(z_k) = A_k \cos(\frac{\pi z_k}{2w_m})$$

where the flux is evaluated at all N points $0 \leq z \leq w_m$ in the z-direction measured from the divertor plate. The A_k are constants that are dependent on the number and placement of points used in the region $[0, w_m]$. For instance, there may be only three grid points inside the width, $z_1, z_2, z_3 \in [0, w_m]$, and the A_k are chosen so that $\Phi(z) = \sum_{k=1}^{3} \Phi(z_k) = I_m$ is satisfied.

Unlike the rocket, there is also now a molecular gas sink specified with total-width w_g (no longer cosine-shaped, this is uniform) on the formerly open end where particles are taken out with flux:

$$\Phi(z) = \frac{1}{4}\sqrt{\frac{8T_g}{\pi m_g}} n_g (1-\alpha) = \frac{1}{4}\sqrt{\frac{8}{\pi m_g}} (1-\alpha) \sum_{k=1}^{N} \sqrt{T_k n_k^2} \approx \sum_{k=1}^{N} \frac{n_k}{1e20} \text{kAmp-equiv}$$

where the sum is over all N points within the region $0 \leq z \leq w_g$ measured from the (other) divertor plate, α is the albedo at the wall and the mass m_g, temperature T_g, and number density n_g are evaluated for the molecular gas. The final approximation is valid for $\alpha = 0.9$ and the assumption used in UEDGE for the molecular gas, $T_g = 0.1$ eV everywhere.

For our test case, we chose recycling at both plates $= 99\%$ with the outer wall sink parameters $\alpha = 0.95$, $w_m = 0.25$. We calculate that the strength of the sink is ≈ -1 kA-equivalent of molecular gas. The electron power gaussian inputs 2 MW with $P_e = C \exp(-\frac{(z-z_1)^2}{2\sigma_z^2} - \frac{(r-r_1)^2}{2\sigma_r^2})$, $\sigma_z = 0.6$, $\sigma_r = 0.1$, $z_1 = 0, r_1 = 1.0$, and C chosen so that the integration over the r-z plane gives 2 MW power. The molecular gas source is 1.0 kA-equivalent of molecular gas. The powers delivered radially and axially are $P_R = 1.97$ kW, $P_Z = 2.35$ MW, $\frac{P_R}{P_Z} \approx .1\%$. Thus the radial power is negligible compared to the axial power, a requirement for an FRC device. Here $\frac{\partial T_e}{\partial r} = \frac{\partial T_i}{\partial r} = 0$ on the outer wall, $T_e = 10 + 20 \exp(-\frac{(z-z_0)^2}{2\sigma_z^2})$, $T_i = 2 + 20 \exp(-\frac{(z-z_0)^2}{2\sigma_z^2})$ on the inner wall, with $\sigma_z = 0.5$ and $z_0 = 0$. Both inner and outer wall density boundaries are Neumann. Contour plots for this new design can be seen in Figure 3.

We obtain typical plasma densities $\approx 2e19 \frac{\text{particles}}{m^3}$ but lower temperatures (15 eV roughly) than initially expected from the previous rocket simulations. It is possible this is because gas no longer escapes and

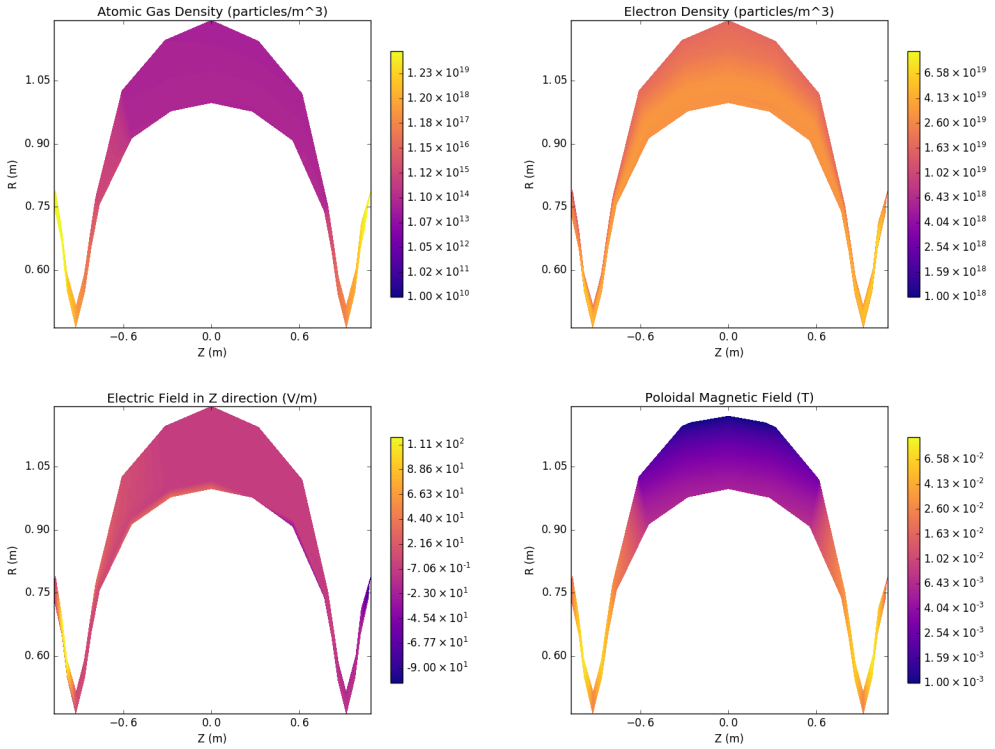

Figure 3: Contour Plots for the SOL region in a FRC device.

instead could create a force balance that slows down the gas in the middle of the grid. The large Electric fields at the sink and source are notably stronger than the corresponding ones for the rocket simulations. For instance, the electric field at the opposite end of the source in the rocket is $\approx 40 - 50\frac{V}{M}$ and here it is $\approx 100 - 120\frac{V}{M}$.

3.6 Gradient Descent

Typically computational methods benefit from having experimental diagnostics and input in order to properly simulate the real physics. While there are no diagnostics for the FRC SOL region at PPPL yet, work has been done to calibrate the UEDGE simulations to a experimental diagnostic in the future. With all boundary conditions set to Dirichlet conditions, the script changes each point in the, for instance, electron temperature boundary condition along the core, by $\pm\epsilon$ and attempts to minimize a particular error with the corresponding experimental profile by using the gradient descent method (Solomon, 2015). The algorithm stops when the error falls below some tolerance τ. For instance, for the radial profile of the electron temperature at $z = 0$,

$$\text{Error} = \sqrt{Average(\frac{|(T_E(r_k, z=0) - T_U(r_k, z=0))|^2}{|T_E(r_k, z=0)|^2})} < \tau$$

Here T_E is the experimental profile for electron temperature (although it can be any variable) and T_U is the UEDGE profile in the same variable. This can be used to match radial or axial profiles in temperature, density, velocity, recycling coefficient, and so on. In order to demonstrate its functionality, below shows the relaxation of a UEDGE profile to the correct experimental profile by this gradient descent method. In this case, the "experimental profile" is an imagined profile of how the electron temperature radial profile should look at $z = 0$. We expect energetic ions with large betatron orbits to heat the SOL relatively uniformly, and a spike of heat at the separatrix from energetic ions at the boundary with small gyro-orbits. In this case, the multi-dimensional gradient method minimizes this error using the variables: $T_e(r = R_{separatrix}, z = 0)$, $T_e(r = R_{max}, z = 0)$, $n_e(r = R_{separatrix}, z = 0)$, $n_e(r = R_{max}, z = 0)$, electron power P_e in MW, half-width of the electron power gaussian σ_e, and radial position of the gaussian r_0. More generally this method can be applied to every point in a profile, like $T_e(r = R_{separatrix}, z)$, but often it is not necessary

and is quite slow. This work is done using OMFIT (Meneghini et al., 2015) since it allows organization of a host of files needed by UEDGE and can submit many UEDGE instances in parallel to a batch system.

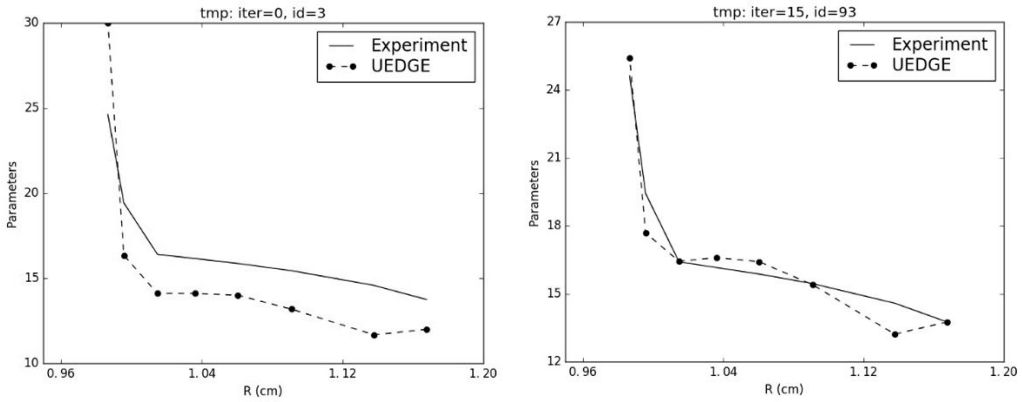

Figure 4: Left: Initial Radial electron temperature profile at z = 0. Right: Same profile after some gradient descent relaxation using only the scalar values of the inner and outer electron wall temperatures at $z = 0$ and the strength of the electron power input.

4 LSP Simulations

LSP is a 3-D electromagnetic parallel particle-in-cell (PIC) code designed for large scale plasma simulations. This code is sophisticated enough to simulate the core region of the FRC. LSP uses an explicit PIC algorithm, with standard particle-advance techniques augmented by a novel energy-conserving push that avoids the so-called Debye-length numerical instability. LSP uses a temporally implicit, noniterative, unconditionally stable electromagnetic field solver and a cloud-in-cell linear interpolation technique between particle locations and grid boundaries. In order to resolve the physics, we require $\Delta t < \omega_p \approx 10$ picoseconds but through testing we found that in order to get the proper physics we needed $\Delta t < 0.1\omega_p \approx 1$ picosecond.

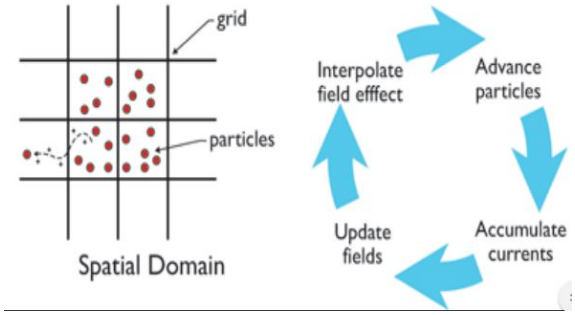

Figure 5: Picture illustrating the PIC method.

The simulation uses only 1 particle-per-cell, with 40 radial cells, 8 azimuthal cells, and 192 axial cells (61440 total cells). Very little change was observed when the particle-per-cell was increased. In centimeters, the spatial extent of the LSP simulation is $r \in [0, 11], z \in [-50, 50], \phi \in [0, 2\pi)$, with typical (non-uniform) grid spacings $\Delta\phi = \frac{\pi}{4}$, $\Delta r_{0\to4} = \frac{1}{6}$, $\Delta r_{0\to11} = \frac{7}{16}$, $\Delta z_{-50\to-25} = \Delta z_{25\to50} = 1$, $\Delta z_{-25\to-10} = \Delta z_{15\to25} = \frac{5}{8}$, and $\Delta z_{-10\to10} = \frac{10}{47}$. Lastly, $\Delta t \approx 1$ picosecond. At this spatial resolution and particle-per-cell, I found it necessary to require $\Delta t < 5$ picoseconds and to require scattering and ionization every timestep (scattering_interval and ionization_interval = 1). There is obvious room for optimization in this regard to reduce the run time of the simulation. A typical simulation takes $\approx$ day on 64 processors. Simulations are usually for 4 μs, during which time the plasma density increases by $\approx$ a factor of 10 before field reversal occurs.

Typical parameters for these runs, including cross-sections and scattering rates, can be found in (D. R. Welch and Glasser, 2010). We repeat it briefly here for clarity and continuity purposes. The RMF antennae are

modeled with a sinusoidal current. The applied magnetic fields from the small- and large bore coils at both ends of the PFRC are precalculated from a magnetostatic solution. Particles striking axial, radial, and FC boundaries are removed from the simulation.

A simulation begins with an $n_e = 10^{11}$ cm^3, $T_e = 4eV$ hydrogen plasma seeded in the Pyrex vessel, along with room-temperature molecular hydrogen with $n_m = 3.4e13$ cm^3. The RMF causes H2 ionization. H2+ is the dominant ion species formed in these relatively short simulations. LSP calculates energy losses by collective radiation, charge exchange, and ionization, as well as conduction and convection to boundaries.

4.1 FRC Formation

Before moving on to other antenna possibilities, we would like to qualitatively reproduce the previous results (D. R. Welch and Glasser, 2010) in order to verify we have proper FRC formation. In figure 6 we can see that the plasma density increases by an order of magnitude, B_z drops below zero, and we obtain the closed field lines.

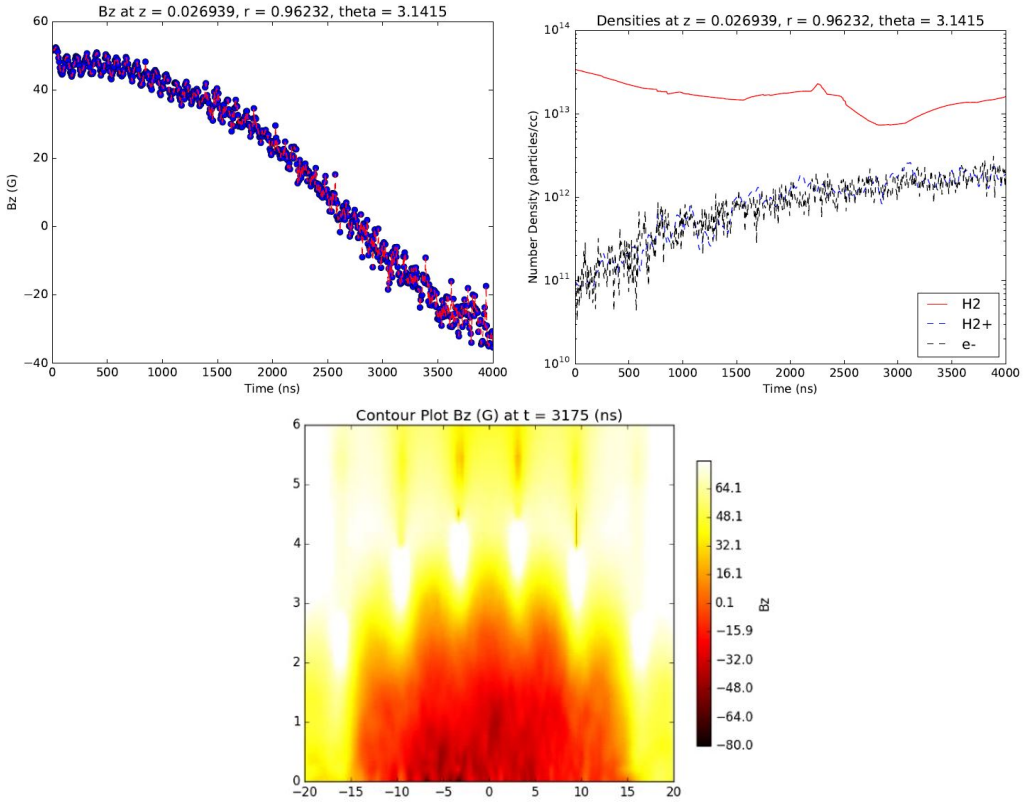

Figure 6: Top: B_z and the plasma densities near $z = 0$ cm, $r = 1$ cm. Bottom: Contour plot in the Z-R plane of B_z illustrating the FRC formation with influence from the six flux conservers.

4.2 Even-Parity RMF

One of the goals of the LSP work is to try and better understand the lack of plasma penetration with even-parity RMF. The resulting plots in figure 7 show that with the same parameters as with the odd parity runs, the densities increase and Bz drops slightly but there is no FRC formation.

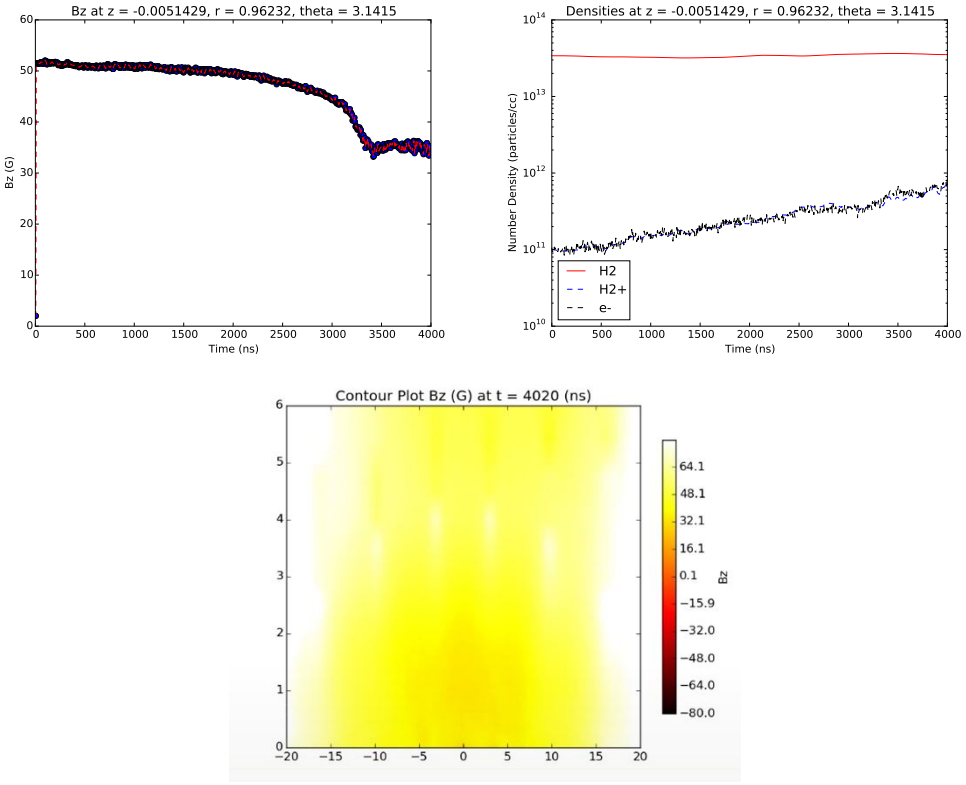

Figure 7: Top: B_z and the plasma densities near $z = 0$ cm, $r = 1$ cm. Bottom: Contour plot in the Z-R plane of B_z illustrating the lack of FRC formation. The densities increase by not quite by an order of magnitude. The axial magnetic field begins to drop but does not get far. The fluctuations on the plots are smaller than before as these runs used more particles-per-cell.

4.3 New Antenna Design

There is interest into whether the RMF antenna can generate the proper FRC formation with only the axial fields. This would reduce the complexity of the FRC design significantly. We can test this by "folding" up the antenna geometry (keeping the current strength, frequency, and phases) as in Figure 8.

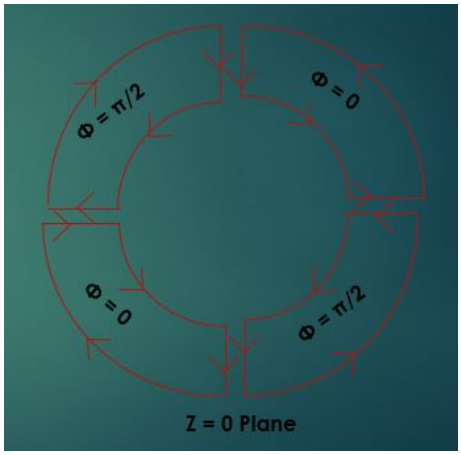

Figure 8: The R-ϕ plane at $z = 0$ displaying the new antenna design with Φ denoting the phase shift of the current drive

This generates axial magnetic fields but not longer generates the large (5-15 Gauss) azimuthal magnetic fields as before. We expect roughly 1% of the strength for B_ϕ and this can be seen in figure 9. However, with this design we see very little magnetic field penetration into the plasma. At first, we thought something was wrong about the simulation. However, after lots of checking, this appears not to be the case. The antenna's B_ϕ field initially appears in the contour plots but quickly dies away. The same thing happens for plots of B_z, B_r, E_r, E_z, and E_ϕ. These fields simply get shielded out by the plasma as the run progresses. After 4μs, the fields in the plasma still have changed very little.

Increasing the number of particles per cell, the grid sizes, and the voltage in the antenna did not qualitatively change these plots. Even with 10x the voltage, a similar story unfolds, although the magnitudes of the magnetic fields are correspondingly larger. A several gauss strength B_ϕ seems necessary for the field reversal, or even for any penetration into the plasma at all. Further work should explain why this is so. Within this parameter space, it looks as though this antenna is not viable for FRC formation.

5 Conclusion

There is still much work to be done in UEDGE and LSP. In UEDGE there is plenty of parameter space to explore and new magnetic geometries to try. My work helps in this regard because it allows us to use UEDGE much more fruitfully. My work gives a prescription to future students on how to get convergence from scratch in UEDGE. This is essential for doing anything new in UEDGE. Moreover, UEDGE can now run as an FRC "power plant", easily make changes to the magnetic geometry, and fit experimental diagnostics. In LSP, there is much to explore as well. My work gives a first look at how FRC formation happens, why it does not happen with even-parity RMF, and how the new antenna design affects this formation. However, future work should further investigate the parameter space of these new antenna designs. Moreover, future work should run LSP with atomic hydrogen included in the model (we did not have access to the necessary interaction files that specify ionization and scattering rates with the other species), with impurities, and with the updated design from the latest FRC.

6 Acknowledgments

I would like to thank Dr. Sam Cohen for his support of me and of this project. Thanks to Olivier Oizacard for teaching me the right ways to use UEDGE (and converge!) as well as switching me over to OMFIT, Eugene

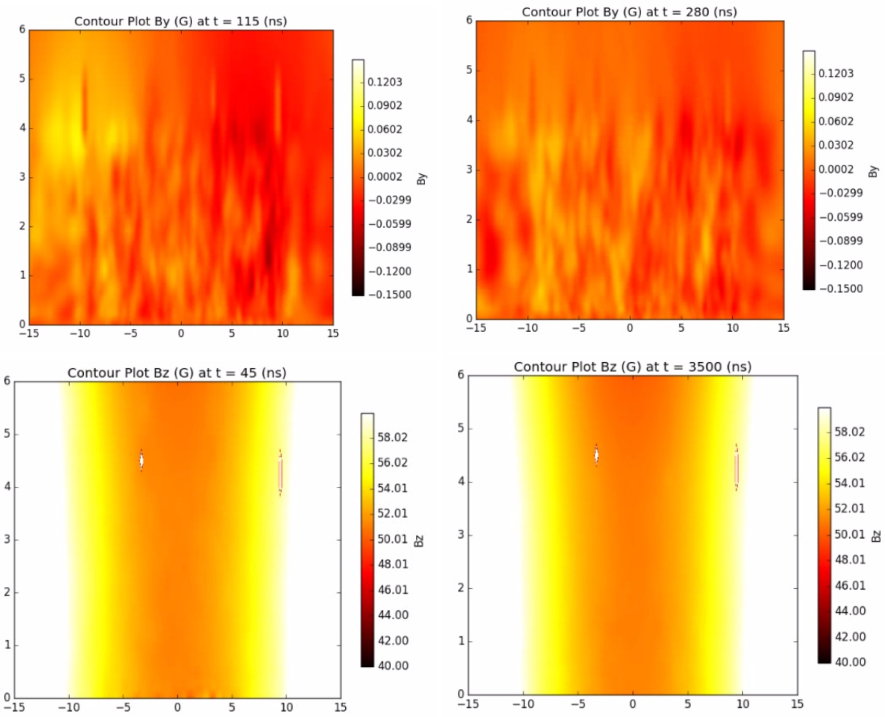

Figure 9: The Z-R plane showing the B_ϕ and B_z field strengths. Top: Initially, the antenna's B_ϕ field is visible in the plasma. By a few hundred nanoseconds later, the antenna field can no longer be seen. Bottom: B_z field essentially unchanged after a few microseconds.

Evans and Andrew Powis for helping me with LSP, Charles Swanson for great suggestions, and Tom Rognlien for UEDGE knowledge.

References

Braginskii, S. (1965). Transport processes in a plasma. *Reviews of Plasma Physics*, I:205.

D. R. Welch, S. A. Cohen, T. C. G. and Glasser, A. H. (2010). Formation of field-reversed-configuration plasma with punctuated-betatron-orbit electrons. *PRL*, 105(1).

McGreivy, N. (2016). Suli report: Uedge simulations of a direct fusion drive frc rocket. *PPPL*, http://w3.pppl.gov/ppst/docs/mcgreivy.pdf.

Meneghini, O., Smith, S., Lao, L., Izacard, O., Ren, Q., Park, J., Candy, J., Wang, Z., Luna, C., Izzo, V., Grierson, B., Snyder, P., Holland, C., Penna, J., Lu, G., Raum, P., McCubbin, A., Orlov, D., Belli, E., Ferraro, N., Prater, R., Osborne, T., Turnbull, A., and Staebler, G. (2015). Integrated modeling applications for tokamak experiments with omfit. *Nuclear Fusion*, 55(8):083008, http://iopscience.iop.org/article/10.1088/0029-5515/55/8/083008/meta.

Olivier Izacard, M. U. (2017). *Gingred, a general grid generator for 2D edge plasma modeling*. Not Yet Published.

Solomon, J. (2015). *Numerical Algorithms*. AK Peters/CRC Press.